Electron Phase Contrast Images of Molecular Detail

By R. D. HEIDENREICH

(Manuscript received March 14, 1966)

Electron phase contrast images with a resolution of at least 2 Å have been obtained using a modified commercial electron microscope. A "phase column" approximation for interpreting such images is briefly discussed and applied to images of graphite, evaporated carbon, and a synthetic polypeptide. Hexagonal features about 5 Å in diameter are attributed to the graphite unit cell imaged by the six first-order prism plane reflections. The image so produced is a next-nearest neighbor representation.

The steady improvement in resolving power of commercial electron microscopes over the past few years has re-awakened considerable interest in the possibilities of directly imaging details of molecular structure. In particular, the phase contrast mechanism based on the Abbé theory of image formation expressed in terms of the Kirchoff diffraction integral has been re-examined using numerical computation methods not in wide use when Scherzer[1] discussed phase image formation. Several theoretical papers[2,3,4,5] dealing with phase contrast images of atom positions have indicated that it should be possible to experimentally obtain such images under the right conditions. The computations all assume a monolayer specimen in the object plane or effectively a single atom approach. This idealized specimen is difficult to realize experimentally and for that reason this brief account is concerned with problems and some results with actual three-dimensional preparations.

High resolution Fourier or "lattice" images of near perfect three-dimensional crystals[6,7] about one-fourth extinction distance thick have become familiar in the last two to three years with image detail exhibited down to 1.8 Å. These have been obtained with crystals for which the total elastic cross section considerably exceeds the inelastic. Tilted illumination has been used which effectively reduces the spherical aberration to zero in one direction. Since it appears that the greatest potential value of high resolution microscopy lies in molecular biology, the sub-

jects of concern here are carbon and high polymers for which the elastic and inelastic cross sections are about the same and the phase contrast situation is, thus, not so favorable.

There are two aspects to high-resolution microscopy: first, an objective lens and instrument capable of point-to-point resolution in the range of interatomic distances and, second, preparation of specimens and interpretation of phase contrast images to obtain intelligible information from the object; i.e., the ability to use the resolving power.

The micrographs displayed here were taken with a modified* Siemens Elmiskop I having improved stability, reduced ac hum, and a focal length shortened from 2.8 to 1.9 mm. The result is a resolving power (point-to-point) with axial illumination of at least 2 Å. In the present configuration the instrument is operated at 80 KV and double condenser with a 200 μ condenser aperture to improve the transverse coherence for phase contrast. Images were recorded photographically at 214,000X and always in focal sequences at 35 Å focal steps.

In the coherent phase-amplitude approximation-to-phase contrast, the intensity $|\Psi|^2$ at a point (x^i,y^i) in the image plane is

$$|\Psi(x^i,y^i)|^2 \cong M^{-2}[1 + |S|^2 + 2S^{\text{real}}] \tag{1}$$

with M the magnification and S^{real} the real part of the phase-amplitude or Kirchoff imaging integral[4,5] over the back focal plane. S is the integral of the product of several terms,† one of which is sin χ with χ the phase relative to the unscattered axial wave.

$$\chi \equiv \chi_{\text{sph.}} + \chi_{\text{astig.}} + \frac{k}{2}\Delta f\beta^2 . \tag{2}$$

Here, $\chi_{\text{sph.}} \approx -(\pi/2\lambda)C_s\beta^4$ is the spherical aberration phase, β the scattering angle, and Δf the defocus from the precise Gaussian image condition. Since $C_s = Cf$, where f is the focal length of the objective lens, a reduction in f reduces the phase distortion due to spherical aberration. The phase shift $\pi/2$ due to scattering is removed from (2) and included in S. In order that the imaging integral have a useful magnitude for an interplanar spacing $d = |g|^{-1}$, the specimen thickness t must be such that

$$\sqrt{\lambda t/2} \ll d \tag{3}$$

to hold down the destructive phase summation over the specimen thick-

* The modifications were volunteered and carried out by Mr. H. Armbruster of Siemens-America. The author is grateful to Mr. Armbruster for his skill, effort and time in improving the instrument.

† A discussion of the various factors involved with three-dimensional objects will be given in a full publication.

ness. Generally, the thinner the object, the better the phase contrast resolution. Objects 50 Å thick or less are desirable which poses problems in preparation and mounting techniques.

An instructive approach to the interpretation of phase contrast detail is to employ the column approximation[8] used so successfully in diffraction contrast. The difference will be in the fact that the transmitted and diffracted beams from the column are recombined at the image plane and that the column will have definite dimensions and symmetry. These dimensions and symmetry are determined by the reciprocal lattice vectors **g** accepted by the objective lens and not subject to undue phase distortion. Since the angle β in (2) for a Bragg reflection is $\beta = \lambda \mid g \mid$, the imaging integral S will have appreciable magnitude in the column for values of Δf and $\mid g \mid$ that bring (2) near $\pi/2$. The column of thickness t will thus have a prismatic cross section with dimensions and symmetry determined by the **g** vectors optimized by defocus Δf for a given spherical aberration coefficient.

For the case of a thin sheet of graphite normal to the optic axis of the objective lens, the electron diffraction pattern consists only of reflections (*hko*). Of these, only the six prism plane reflections at 2.13 Å are used by the objective lens to produce an image without undue phase distortion. Shorter spacings are presently seriously "garbled" by both spherical aberration and uncorrected astigmatism. Micrographs taken with and without a 100 μ objective aperture, which passes the prism plane reflections, are very similar. The result is a phase contrast column of thickness t and hexagonal cross section about 5 Å in diameter as depicted in Fig. 1. The relation between the minimum crystallographic unit cell and the column cross section is evident in Fig. 1. Since no information on the shorter interatomic distances reaches the image plane, the cross section is that for a "next-nearest neighbor cell". The nearest neighbor cell would be essentially a benzene ring shown by the dash lines in Fig. 1. It is noted that the information available to the image plane recognizes only four atoms in the cross section of the column whereas there are ten carbon atoms in the structure.

The column approach just discussed is highly useful in interpreting the micrograph of graphite in Fig. 2. The size of the hexagonal "cells" in Fig. 2 is about 5 Å as expected on the basis of Fig. 1. Inelastic scattering and some damage to the thin graphite due to cleaving and mounting act to degrade the delineation of the image of the cells.

The high "noise" level familiar in evaporated carbon substrates becomes understandable from this point of view. A typical high resolution micrograph of a thin carbon substrate is displayed in Fig. 3. In the circled

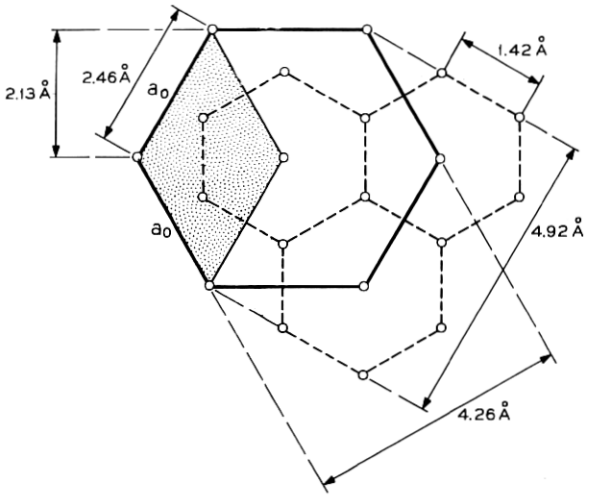

Fig. 1 — Hexagonal array of atoms in a single graphite layer. The unit cell of side $a_0 = 2.46$ Å ($c = 6.7$ Å) is shown cross-hatched. The hexagonal cell shown by the heavy lines is the one defined by the six prism plane reflections at 2.13 Å or the next-nearest neighbor cell.

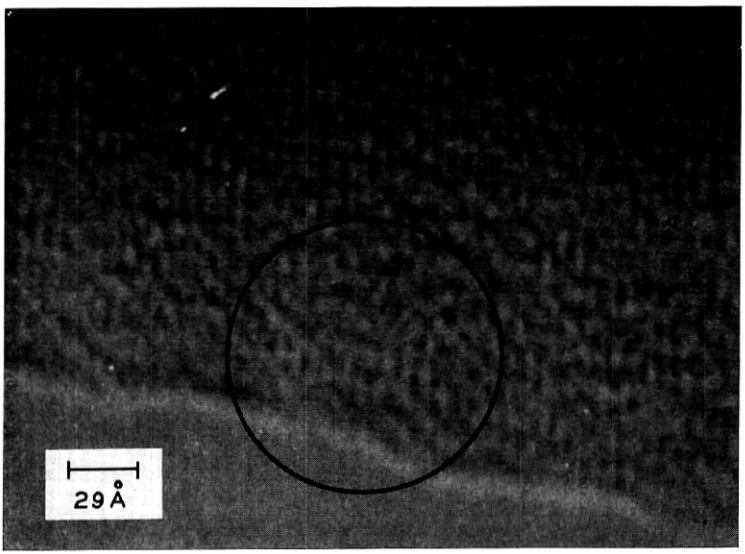

Fig. 2 — Phase contrast micrograph of a cleaved graphite sheet using the prism plane reflection and showing the hexagonal cells of Fig. 1 about 5 Å in diameter. The defocus is about 100 Å to the focal length side. (80 *KV*, 200 μ condenser aperture. No objective aperture. Electronic magnification 214,000×.)

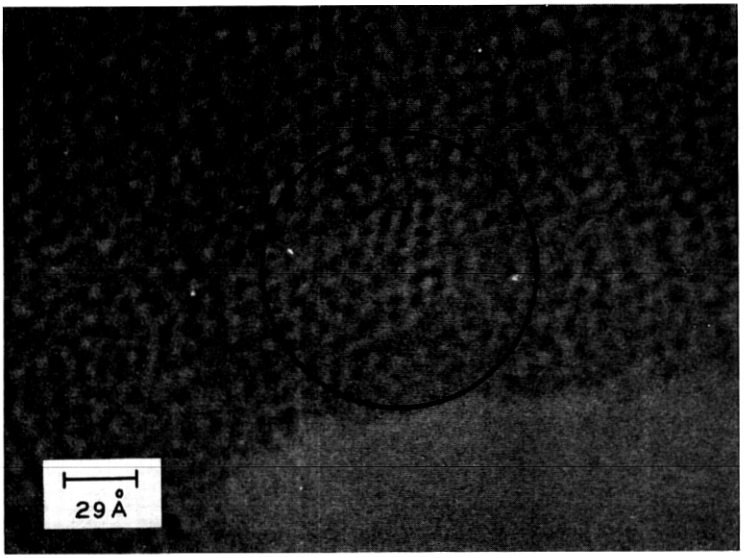

Fig. 3 — Micrograph of an evaporated carbon substrate displaying the hexagonal cells in the circled area where the c-axis is normal to the sheet. The crystallite size in this region is around 20 Å. Neighboring regions are at different orientations.

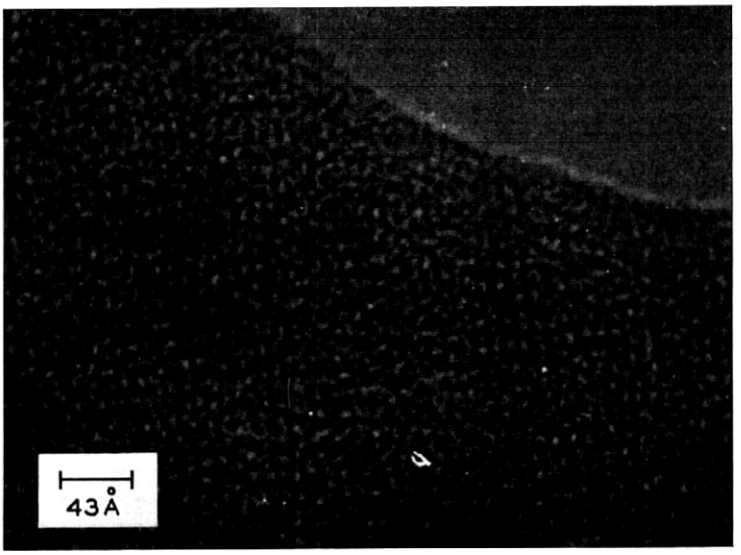

Fig. 4 — Micrograph of a thin film (≈60 Å) of the synthetic polypeptide poly-γ-benzyl-L-glutamate at lower magnification showing the extent of ordered structure seen by phase contrast. Hexagonal cells such as those of Fig. 3 are found scattered through the image.

region are several hexagonal cells about 5 Å in diameter taken to be due to a small graphite crystallite only a few cells in extent oriented with the c-axis normal to the film. Neighboring areas are composed of other crystallites unsuitably oriented to produce the prism plane reflections. So called amorphous carbon is well approximated by randomly oriented graphite crystallites only a few cells in extent. The structure seen in carbon films is thus actually "graphite noise".

All the polymer films and filaments examined under these conditions show phase contrast structure. Although the use of cold surfaces about the object holder reduces contamination they do not completely remove it. In addition, most polymers suffer radiation damage by 80 KV electrons which leads to the appearance of a diffuse diffraction ring at about 2.1 Å. Consequently, there can be some question as to the origin of hexagonal cells seen in the polymers. There is sufficient detail in such images, however, differing from that seen in Fig. 3 that the images cannot be regarded as just due to carbon. The micrograph in Fig. 4 is a phase image of a thin film of poly-γ-benzyl-L-glutamate (a synthetic polypeptide) at about half magnification of the preceding figures. The ordered structure in the image is evident, but at present the details have not been explained. The α-helix is about 12 Å in diameter so that a single chain should be easily seen if it were isolated. The chains must, therefore, be packed together in Fig. 4 and may be cross-linked which greatly increases the difficulty in interpretation.

From a number of micrographs such as Fig. 4, it appears that if phase contrast high resolution microscopy is to be useful for polymers and biological molecules, techniques of preparing specimens to give isolated chains must be developed. The phase image of an isolated chain should be quite amenable to interpretation using the column concept.

REFERENCES

1. Scherzer, O., J. Appl. Phys. *20,* 1949, p. 20.
2. Hoppe, W., Naturwissenshaften, *48,* 1961, p. 736.
3. Lenz, F., Optik, *21,* 1965, p. 489.
4. Heidenreich, R. D. and Hamming, R. W., Numerical Evaluations of Electron Image Phase Contrast, B. S. T. J., *44,* 1965, p. 207.
5. Eisenhandler, C. and Siegel, B. M., J. Appl. Phys., Feb., 1966.
6. Komoda, T., J. Electron Microscopy, *14,* 1965, p. 128.
7. Komoda, T., Optik, *21,* 1964, p. 93.
8. Hirsch, P. B., Howie, A., Nicholson, R. B., Pashley, D. W., and Whelan, M. J., *Electron Microscopy of Thin Crystals,* Butterworths, London, 1965, p. 157.